JOURNAL OF SOLID STATE CHEMISTRY 69, 109–115 (1987)

Oxygen Potentials for the Oxidation of Rare Earth Oxysulfides to Oxysulfates

K. T. JACOB,* R. AKILA,*,† AND A. K. SHUKLA‡

*Department of Metallurgy, †Materials Research Laboratory, and ‡Solid State and Structural Chemistry Unit, Indian Institute of Science, Bangalore 560 012, India

Received May 28, 1986; in revised form October 30, 1986

The equilibrium oxygen potentials corresponding to the oxidation of rare earth oxysulfides to their respective oxysulfates are measured in the temperature range 900 to 1480 K using the solid-state cell Pt, Ni + NiO/(CaO)ZrO_2/R_2O_2S + $R_2O_2SO_4$, Pt, where R = La, Pr, Nd, Sm, Eu, Gd, Tb, or Dy. The reference electrode consisting of a mixture of Ni + NiO is selected as its oxygen potential lies close to those of the rare earth systems studied here. At a constant temperature, the oxygen potentials for the oxidation of the oxysulfides to oxysulfates are found to increase monotonically with the atomic number of the rare earth element. The "second law" enthalpy change for the oxidation reaction also shows a similar trend, albeit a larger uncertainty. Based on the empirical trend, the changes in the standard Gibbs' energy accompanying the conversion of oxysulfides of Ho, Er, and Tm to their oxysulfates are estimated. The higher polarizing powers of the heavier trivalent rare earth ions appear to destabilize the relatively open structure oxysulfates more than the close-packed oxysulfides.

Introduction

Thermodynamic data on rare earth oxysulfides at high temperatures are useful for optimizing the conditions for rare earth treatment of iron and steel. Rare earth additions are used for deoxidation and desulfurization and control of inclusion morphology in steel and graphite morphology in cast iron. Rare earth oxysulfides are also used as host material for phosphors. Systematic studies on the thermodynamic properties of these oxysulfides are, however, limited. The structures of rare earth oxysulfides and oxysulfates have been discussed in the literature (*1–3*).

Phase relations in the ternary R_2O_3–R_2S_3–SO_3 system at approximately 1200 K are represented in Fig. 1. At a fixed temperature, the chemical potentials of certain gaseous species are unambiguously defined by condensed phase equilibria as shown in the diagram. In the three phase regions, all chemical potentials are fixed. Equilibrium between $R_2(SO_4)_3$ and $R_2O_2SO_4$ or $R_2O_2SO_4$ and R_2O_3 defines unique partial pressures of SO_3 at a fixed temperature. The ratio of partial pressures of sulfur to oxygen is defined when R_2O_3 coexists with R_2O_2S or R_2O_2S coexists with R_2S_3. The oxysulfide and oxysulfate in equilibrium fix the oxygen chemical potential, which can be measured by a solid-state cell.

Thermogravimetric studies (*4–7*) have indicated qualitatively the sequence of steps in the oxidation of rare earth oxy-

0022-4596/87 $3.00

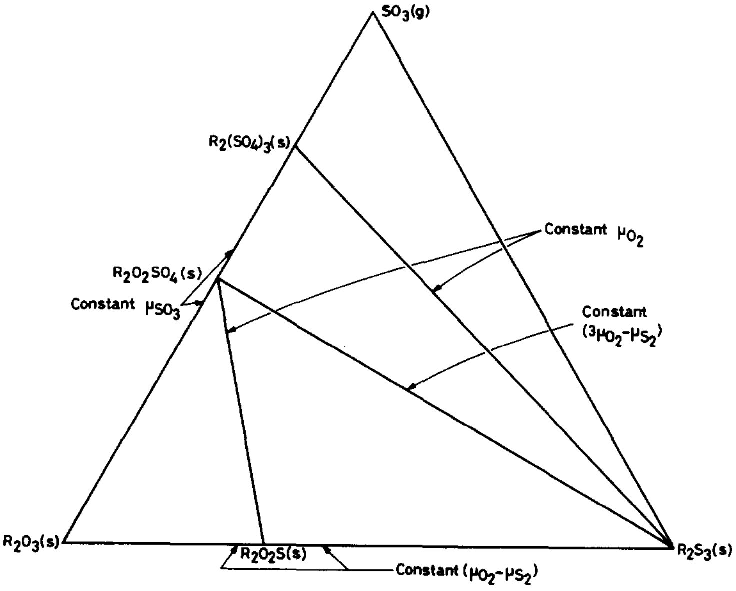

FIG. 1. Phase relations in the ternary R_2O_3–R_2S_3–SO_3 system, where R represents a light rare earth element.

sulfides in air. They oxidize to their respective oxysulfates at high temperatures. The oxysulfates decompose to the respective oxides on further heating in air. The decomposition of oxysulfates may start before the oxidation of the oxysulfide is complete. The heavier rare earth oxysulfates decompose to oxides at temperatures lower than those of the lighter elements.

The oxygen chemical potentials established by the equilibrium between the rare earth oxysulfide and the corresponding oxysulfate have been measured recently by Dwivedi and Kay (*8*) and Fukatsu *et al.* (*9*). Dwivedi and Kay used a calcia-stabilized zirconia (CSZ) solid electrolyte with a three-phase mixture of the rare earth oxide, oxysulfide, and oxysulfate to uniquely fix the partial pressures of all gaseous species at the test electrode. The reference electrode was air in contact with platinum. In the temperature range 1000–1500 K, they determined the standard free energy changes for the conversion of rare earth oxysulfides to oxysulfates. The disadvantage in using a three-phase mixture is the extended time required for equilibration.

Fukatsu *et al.* (*9*) used a test electrode consisting of a two-phase mixture of the oxysulfide and oxide or oxysulfide and oxysulfate, in equilibrium with an S–O gas mixture at 1 atmosphere total pressure. The oxygen potential was measured with a CSZ electrolyte having an air reference electrode. From the measured oxygen potential, the gas composition was numerically computed using thermodynamic data for gaseous species in the S–O system available in the literature, subject to the constraint of 1 atmosphere total pressure. The sulfur and oxygen potentials were then used in the calculation of the standard free energies of formation of the rare earth oxysulfides and oxysulfates. As data for a large number of species, viz., SO_3, SO_2, S_2O, S, S_2, S_3, S_4, S_5, S_6, S_7, S_8, O, O_2, and O_3, are used to compute the gas composition, cumulative errors in the free energies of formation of the rare earth oxysulfides/oxysulfates may be relatively large.

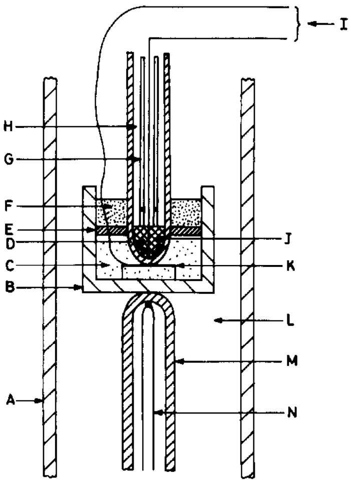

FIG. 2. Cell arrangement for measuring the oxygen partial pressure coexisting with an R_2O_2S + $R_2O_2SO_4$ mixture (R = La, Pr, Nd, Sm, Eu, Gd, Tb, or Dy). (A) Outer tube, Al_2O_3, (B) (CaO) ZrO_2 crucible, (C) Ni + NiO mixture, (D) (CaO) ZrO_2 tube, (E) layer of NiO, (F) (CaO) ZrO_2 powder, (G) support tube, Al_2O_3, (H) quasi-static argon atmosphere, (I) platinum leads, (J) R_2O_2S + $R_2O_2SO_4$ mixture, (K) porous platinum sheet, (L) flowing argon gas, (M) thermocouple sheath, Al_2O_3, (N) Pt/Pt–13% Rh thermocouple.

Experimental Aspects

Materials

The rare earth oxysulfides (R_2O_2S) are prepared by hydrogen reduction of corresponding sulfates $R_2(SO_4)_3$ at 1000 K. The oxysulfates are prepared by heating anhydrous sulfates in air between 1073 and 1223 K. The higher temperatures are used for the lighter rare earth elements.

The sulfate crystals are obtained by evaporation from a solution of oxides in 60% sulfuric acid. The sulfates are dehydrated by heating at 900 K. The starting oxides are 99.9% pure. The main impurities are the other rare earth elements.

Apparatus and Procedure

The experimental arrangement used for the emf measurements is shown in Fig. 2. It is similar to that used earlier by Jacob and Iyengar (*10*) for the study of sulfide–sulfate equilibria involving alkaline earth elements. The cell consists of a fully stabilized zirconia tube (15 mole% CaO) with an equimolar mixture of R_2O_2S and $R_2O_2SO_4$ packed into it. Electrical contact is through a Pt lead embedded in the mixture. The outside of the zirconia tube is kept in contact with a reference electrode mixture of Ni + NiO, in the molar ratio 2 : 1. A Pt lead spot welded on a Pt foil serves to establish electrical contact to this electrode. Both electrical contacts are kept within the constant temperature zone of the furnace to eliminate thermoelectric effects. X-ray diffraction of the R_2O_2S + $R_2O_2SO_4$ electrode mixture before and after the experiment showed no change, suggesting that mutual solubility between the phases is negligible.

The experiments are performed with argon flowing in both compartments of the tube. The inside of the solid electrolyte tube is initially flushed with argon gas. The flow rate is reduced to 10 ml/min, during the experiment, so that the argon atmosphere over the test electrode is virtually static. The emfs are found to be independent of the flow rates of argon in both chambers. The reversibility of the cell was checked by passing small currents (150 μA for 5 min) and verifying that the emf returned to the original value before titration. The emfs are reproducible after temperature cycling. The cell temperature is measured to 1 K by a Pt/Pt–13% Rh thermocouple kept in contact with it. With a symmetric cell arrangement,

$$\text{Pt, Ni} + \text{NiO/(CaO)ZrO}_2\text{/Ni} + \text{NiO, Pt,} \tag{I}$$

the cell emf in the temperature range 900–1500 K is ± 0.15 mV, thus verifying the absence of any significant thermal gradient

TABLE I

TEMPERATURE DEPENDENCE OF CELL ELECTROMOTIVE FORCE AND OXYGEN POTENTIALS CORRESPONDING TO THE RARE EARTH OXYSULFIDE/OXYSULFATE EQUILIBRIA

System R	E^a (mV) (±0.2)	$\Delta\mu_{O_2}{}^b$ (J/mole) (±500)
La	23.7 − 0.0182 T	−459,170 + 162.77 T
Pr	47.8 − 0.0227 T	−449,870 + 161.03 T
Nd	49.1 − 0.0195 T	−449,360 + 162.26 T
Sm	54.4 − 0.0179 T	−447,320 + 162.88 T
Eu	63.0 − 0.0227 T	−444,000 + 161.03 T
Gd	63.8 − 0.0214 T	−443,690 + 161.53 T
Tb	60.8 − 0.0173 T	−444,850 + 163.11 T
Dy	73.9 − 0.0262 T	−439,790 + 159.68 T
Ho	—	(−441,200 + 161.30 T)[c]
Er	—	(−440,660 + 161.28 T)[c]
Tm	—	(−440,220 + 161.29 T)[c]

[a] For the cell Pt, Ni + NiO/CaO–ZrO$_2$/R_2O_2S + $R_2O_2SO_4$, Pt.

[b] For the reaction $\frac{1}{2}\langle R_2O_2S\rangle + (O_2) \rightarrow \frac{1}{2}\langle R_2O_2SO_4\rangle$.

[c] Estimates based on the empirical trend observed in this study.

across the cell and the associated thermoemf.

Results

The emfs of the cells

$$\text{Pt, Ni + NiO/(CaO)ZrO}_2/R_2O_2S + R_2O_2SO_4\text{, Pt,} \quad \text{(II)}$$

where R = La, Pr, Nd, Sm, Eu, Gd, Tb, or Dy, are measured in the temperature range 900 to 1480 K. The right-hand electrode is positive. The Ni + NiO reference electrode is selected for this study because its oxygen potential is close to those of the systems being measured. This results in a smaller gradient of oxygen chemical potential across the cell, so that the electrochemical flux of oxygen from the higher potential electrode to the lower potential electrode due to the trace electronic conductivity of the solid electrolyte and the consequent polarization of the electrodes are minimized. Since the measured emfs are less than 50 mV, they could be measured to ±0.2 mV.

The equations relating the cell emf to temperature obtained by least-mean-squares regression analysis are shown in Table I for the various rare earth systems. With increasing atomic number of the rare earth element, the upper temperature limit for measurements is successively lowered because of the instability of the oxysulfate. Once the decomposition temperature is exceeded, the emfs are not reproducible. The measured reversible emfs are plotted as a function of temperature for the various rare earth systems in Fig. 3.

The cathodic reaction in the electrochemical cell can be represented as

$$R_2O_2SO_4 + 8e^- \rightarrow R_2O_2S + 4O^{2-}. \quad (1)$$

The anodic reaction is

$$\text{Ni} + O^{2-} \rightarrow \text{NiO} + 2e^-. \quad (2)$$

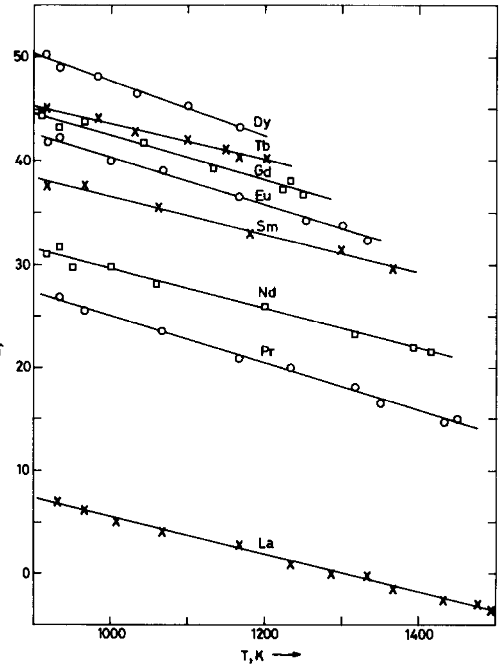

FIG. 3. Temperature dependence of emf of cell Pt, Ni + NiO/(CaO)ZrO$_2$/R_2O_2S + $R_2O_2SO_4$, Pt, where R = La, Pr, Nd, Sm, Eu, Gd, Tb, or Dy.

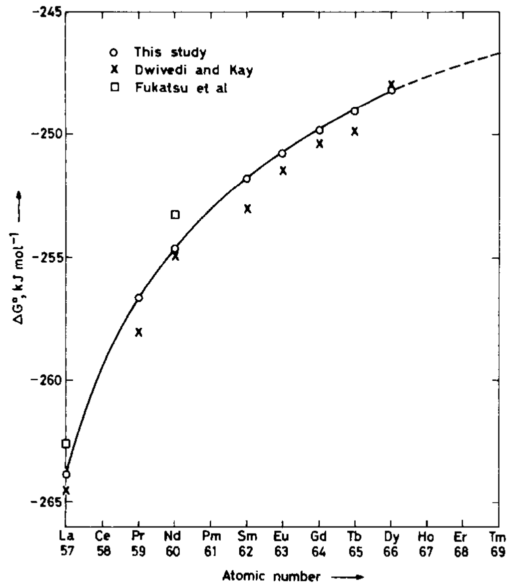

FIG. 4. The standard Gibbs' energy change for the reaction $\frac{1}{2}R_2O_2S(s) + O_2(g) \rightarrow \frac{1}{2}R_2O_2SO_4(s)$ at 1200 K plotted as a function of rare earth atomic number.

The overall cell reaction is

$$\tfrac{1}{2}\langle R_2O_2SO_4\rangle + 2\langle \mathrm{Ni}\rangle \rightarrow \tfrac{1}{2}\langle R_2O_2S\rangle + 2\langle \mathrm{NiO}\rangle, \quad (3)$$

where ⟨ ⟩ represents the solid state. The free energy change for reaction (3) is given by

$$\Delta G^\circ = -nFE, \quad (4)$$

where $n = 4$ is the number of electrons involved in the cell reaction, F is the Faraday constant, and E is the emf associated with reaction (3). By combining this with the standard free energy of formation of NiO given by (*11*),

$$\Delta G^\circ_f\{\mathrm{NiO}\} = -234{,}160 + 84.89\ T\ \mathrm{J/mole}, \quad (5)$$

the standard free energy change or the oxygen potential for the oxidation of the rare earth oxysulfide to oxysulfate,

$$\tfrac{1}{2}\langle R_2O_2S\rangle + (O_2) \rightarrow \tfrac{1}{2}\langle R_2O_2SO_4\rangle, \quad (6)$$

is obtained. Here ( ) denotes the gas phase. The chemical potentials of oxygen are also summarized in Table I. The values for Ho, Er and Tm have been estimated based on empirical trends observed in this study.

Discussion

The standard Gibbs' energy change associated with reaction (6) at 1200 K is shown as a function of rare earth atomic number in Fig. 4. The values obtained by Dwivedi and Kay (*8*) are lower by 0 to 1.3 kJ, while those of Fukatsu *et al.* (*9*) are higher by 1.3 kJ for La and Nd. The agreement between the three investigations is remarkable. The results obtained in this study show a smooth variation with atomic number. The curve can be extended to heavier rare earth ions and the oxygen potentials for the oxidation of the oxysulfides to oxysulfates can be estimated.

The variation of the standard enthalpy change for reaction (6) obtained in this study with atomic number, shown in Fig. 5, appears to follow the same trend as the Gibbs' energy, albeit with a larger scatter. The absolute uncertainty in the enthalpy change calculated from the results of this study varies from ±1350 J/mole for La to ±1600 J/mole for the Dy system. The uncertainty is progressively larger for heavier rare earth elements because of the smaller temperature range available for measurement. The results of Dwivedi and Kay (*8*) and Fukatsu *et al.* (*9*) show larger scatter. The results of Dwivedi and Kay exhibit a double-humped behavior. Since the oxidation state of the rare earth ion is not altered during the oxidation of the oxysulfide to the corresponding oxysulfate, and the ionic radius for the trivalent state decreases monotonically with atomic number, there is no obvious theoretical justification for the trend exhibited by the results of Dwivedi and Kay. It is more likely that the error in the second law enthalpies obtained from

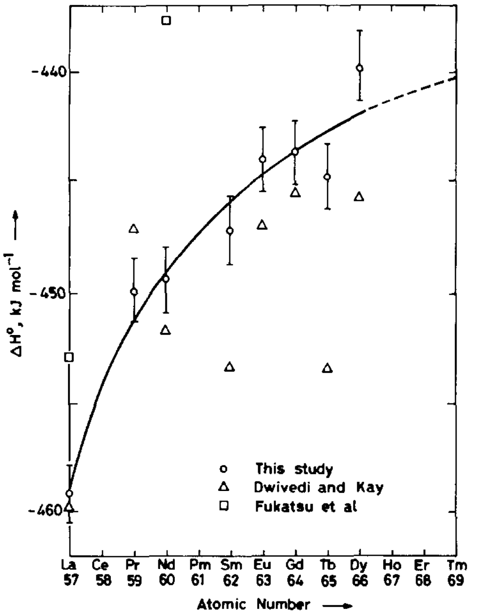

FIG. 5. Variation of ΔH° for the oxidation of oxysulfides to oxysulfates with atomic number of the rare earth element.

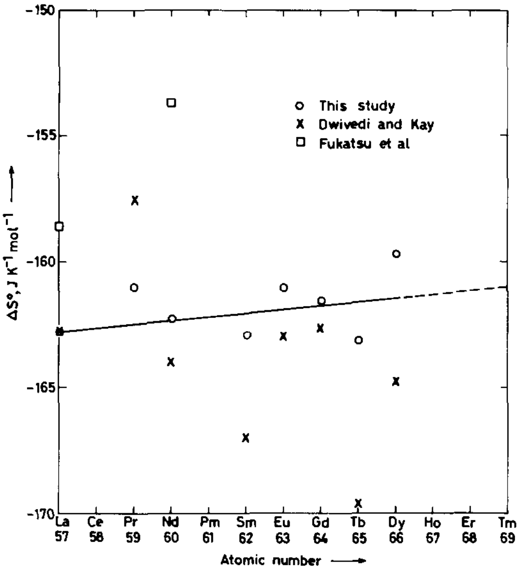

FIG. 6. Dependence of the standard entropy change for the oxidation of rare earth oxysulfides to oxysulfates on atomic number of the rare earth element.

their study is too large (±6 kJ/mole) to reveal systematic trends.

The standard entropy change for reaction (6) obtained in this study is compared with the results of Dwivedi and Kay and Fukatsu *et al.* in Fig. 6 as a function of atomic number. Again the data of Dwivedi and Kay do not show the same trend, while the data of Fukatsu *et al.* suggest a steeper increase with atomic number. The values for the enthalpy and entropy change correspond to the mean temperature of measurement for each system. These values require confirmation by calorimetric techniques.

The trends in Figs. 4 and 5 show that the stability of the oxysulfate relative to the oxysulfide decreases with increasing atomic number or decreasing atomic diameter of the trivalent rare earth ion. The polarizing power of the rare earth ion increases with decreasing radius. The higher polarizing power of the heavier trivalent rare earth ions appears to destabilize the relatively open structured oxysulfates more than the close-packed oxysulfides. It would be worth examining how the stability of the rare earth oxysulfides relative to that of the corresponding oxides will vary with atomic number.

Acknowledgments

The authors are grateful to the Board of Research in Nuclear Sciences, Department of Atomic Energy, Government of India for financial support. The authors wish to thank Mr. N. Venugopal Rao for assistance in the preparation of this manuscript.

References

1. W. H. ZACHARIASEN, *Acta Crystallogr.* **2**, 60 (1949).
2. P. LARUELLE, *Ann. Chim. (Paris)* **7**, 119 (1982).
3. R. BALLESTRACCI AND J. MARESCHAL, *Mater. Res. Bull.* **2**, 993 (1967).
4. J. W. HAYES AND J. J. BROWN, *J. Electrochem. Soc.* **111**, 1060 (1968).

5. R. D. Baybarz, J. A. Fahey, and R. G. Haire, *J. Inorg. Nucl. Chem.* **36,** 2023 (1974).
6. L. Ozawa, *J. Electrochem. Soc.* **124,** 413 (1977).
7. M. Leskela and L. Niinisto, *J. Therm. Anal.* **18,** 307 (1980).
8. R. K. Dwivedi and D. A. R. Kay, *Metall. Trans., B* **15,** 523 (1984).
9. N. Fukatsu, N. Shidawara, and Z. Kozuka, *J. Electrochem. Soc.* **132,** 2258 (1985).
10. K. T. Jacob and G. N. K. Iyengar, *Metall. Trans., B* **13,** 387 (1982).
11. B. C. H. Steele, *in* "Electromotive Force Measurements in High Temperature Systems" (C. B. Alcock, Ed.), pp. 3–28, The Institution of Mining and Metallurgy, London (1968).